Teknomekanik, Vol. 9, No. 2, 2026, pp. 256-271
e-ISSN: 2621-8720 p-ISSN: 2621-9980

Design, control, and development of a low-cost single-tilt-rotor Tricopter

Fahmizal[1], Ahmad Jaelani Sidik[1], Priyova Muhammad Rafief[1], Hari Maghfiroh[2*], Mariusz Jablonski[3], and Piotr Borkowski[3]

[1] Department of Electrical Engineering and Informatics, Vocational College, Universitas Gadjah Mada, **Indonesia**
[2] Department of Electrical Engineering, Universitas Sebelas Maret, **Indonesia**
[3] Department of Electrical Engineering, Lodz University of Technology, **Poland**

*Corresponding Author: hari.maghfiroh@staff.uns.ac.id
Received: 11 January 2026; *Revised:* 25 May 2026; *Accepted:* 06 June 2026

Cite this https://doi.org/10.24036/teknomekanik.v9i2.53172

Abstract: This paper presents the design, implementation, and experimental validation of a low-cost PID-based attitude control system for a single-tilt-rotor tricopter. The proposed platform employs a Y-shaped frame configuration with a servo-driven tail-tilt mechanism and is implemented using a low-cost ATmega328P microcontroller and GY-88A IMU sensor. A PID controller was used for inner-loop attitude stabilization of roll, pitch, and yaw motions due to its low computational complexity and suitability for resource-constrained embedded systems. The PID gains were obtained through manual tuning using a tricopter test-bed rig under disturbance-free conditions and experimentally evaluated under both static and dynamic wind disturbances. Under a static wind disturbance of 7.2 m/s, the roll and pitch mean absolute error (MAE) values reached 0.977° and 4.826°, respectively, while dynamic disturbance testing produced MAE values of 0.823° for roll and 2.094° for pitch. Outdoor flight tests resulted in MAE values of 1.133° for roll and 1.831° for pitch. The experimental results demonstrated that the proposed low-cost tricopter platform can maintain stable attitude control under the evaluated disturbance conditions and outdoor flight scenarios. The study highlights the feasibility of implementing reliable tricopter stabilization using computationally lightweight PID control on inexpensive embedded hardware.

Keywords: low-cost UAV development; PID-based attitude control; single-tilt-rotor UAV; tricopter

1. Introduction

Unmanned aerial vehicles (UAVs) are aircraft capable of remote piloting or autonomous operation, and they have become essential tools in both civilian and military applications [1][2][3]. In recent years, UAVs have played a significant role in the digital transformation of cities and in promoting sustainable urban development. Their applications include disaster response [4], air quality monitoring [5], global mapping [6], and chemical, biological, radiological, and nuclear (CBRN) area surveillance [7]. UAVs can generally be categorized into two main types: fixed-wing and rotary-wing aircraft. Among rotary-wing configurations, vertical take-off and landing (VTOL) platforms have attracted significant interest due to their ability to operate without runways [8][9]. These aircraft, commonly known as multi-copters, include quadcopters, hexacopters, and tricopters, which are classified according to the number of rotors [10][11]. A comprehensive overview of multi-copter systems is presented in [12].

A tricopter employs three primary brushless motors, each driving a propeller. Key design considerations include stability, mechanical simplicity, lightweight structure, and cost-effectiveness. Compared to quadcopters, tricopters offer improved maneuverability, reduced

weight, and simpler structural layout, making them suitable for low-cost UAV applications. Tricopters offer greater maneuverability and lower cost than quadcopters [13]. They can also achieve longer flight times due to reduced power demand and aerodynamic simplicity [14]. A T-shaped tricopter stabilized using the Newton–Euler model and a nonlinear control [15] was introduced; a hybrid tricopter design combining VTOL and fixed-wing features [16] was proposed to enhance endurance. Papachristos et al. [17] applied an LQR-based optimal tracking controller to a longitudinal thrust-vectoring tri-tilt-rotor UAV, demonstrating improvements in trajectory precision. These studies highlight the growing scientific interest in tricopters and tilt-rotor variants due to their maneuverability and mechanical efficiency.

To regulate tricopter stability, various control techniques, both linear and nonlinear, have been investigated. The PID controller remains the most widely adopted approach due to its simplicity, low computational burden, and reliable performance [18][19][20]. More advanced methods such as fuzzy logic control [21][22], quaternion feedback control (QFB), and model predictive control (MPC) [23][24] have also been explored to improve stability and dynamic response. In addition, industrial balancing and correction algorithms have been adapted for UAV attitude stabilization [25]. However, many of these approaches are primarily validated through simulations or implemented using relatively high-performance embedded processors. Consequently, their practical implementation on low-cost hardware platforms remains relatively limited.

Furthermore, existing tricopter studies often focus only on mechanical design, control algorithms, or aerodynamic analysis in isolation. Only a limited number of studies integrate controller implementation and full hardware development into a single experimentally validated low-cost tricopter platform. In particular, experimental validation under real-world external disturbances, such as wind effects, is still rarely discussed for single-tilt-rotor tricopter configurations operating with inexpensive microcontrollers. Therefore, this study addresses the gap by integrating two main aspects: attitude control and low-cost hardware development of a single-tilt-rotor tricopter. A PID-based attitude control strategy is implemented to maintain roll, pitch, and yaw stability under disturbance conditions. In addition, a compact and affordable tricopter platform is developed using an ATmega328P microcontroller and GY-88A IMU to experimentally validate the proposed approach under test-bed and outdoor flight conditions.

The main novelty of this work lies in the development of an experimentally validated low-cost single-tilt-rotor tricopter that integrates embedded PID control and practical hardware implementation on a resource-constrained microcontroller platform. Unlike many previous studies that rely heavily on simulations or expensive flight controllers, the proposed system demonstrates stable attitude control performance under controlled disturbances and in outdoor flight conditions using inexpensive and widely accessible components. The contributions of this study are summarized as follows:

1. Design and implementation of a computationally efficient PID-based attitude controller for embedded real-time stabilization;
2. Development of a low-cost single-tilt-rotor tricopter platform using ATmega328P and GY-88A IMU hardware;
3. Experimental validation under static and dynamic wind disturbances using a dedicated test-bed rig;
4. Outdoor flight testing to evaluate practical attitude stabilization performance under real operating conditions.

2. Material and methods

2.1 Mechanical design

The mechanical design of the tricopter integrates multiple components into a unified structure, including the upper and lower bases, and arms that accommodate the electronic elements. The upper base houses the flight controller, receiver, and telemetry module. A vibration damper is employed to mitigate disturbances that could affect the IMU sensor and to protect the flight controller from excessive vibration. This is crucial for maintaining the accuracy of IMU readings and minimizing the risk of overshooting in the tricopter's attitude control. The lower base contains the power distribution board, which distributes power from the battery to the electronic speed controllers (ESCs), as well as the batteries and landing gear. Each arm incorporates ESCs, motor mounts, and a servo-driven tail mechanism. The overall mechanical configuration of the tricopter is shown in Figure 1.

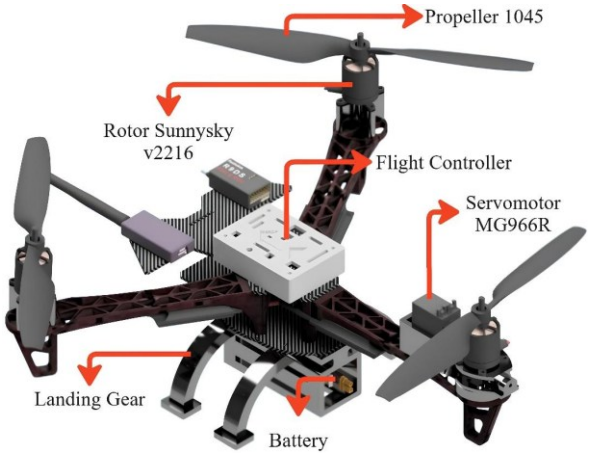

Figure 1. Tricopter mechanical design

The test rig shown in Figure 2 is designed to analyse the tricopter's motion during roll, pitch, and yaw maneuvers. This device enables PID gain tuning and the evaluation of stability improvements without requiring direct flight tests. It also ensures that the tricopter remains stable when subjected to disturbances across different orientations. It provides three degrees of freedom (DoF), allowing manipulation of roll, pitch, and yaw. The test rig consists of two main components: the support frame and the housing. The support frame is constructed from interconnected pipes for structural stability, while the housing comprises simple pipes connected on both sides to accommodate the tricopter. The overall dimensions of the rig are 102 cm in length, 68 cm in width, and 120 cm in height.

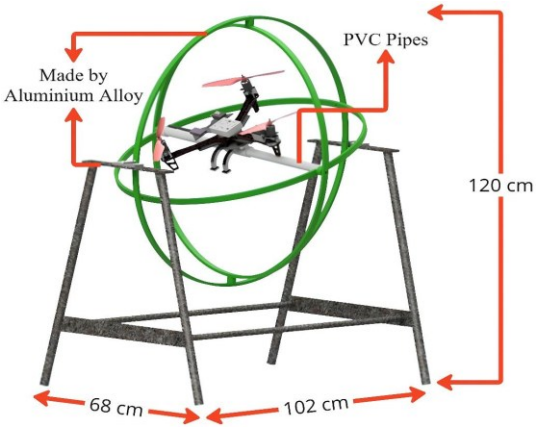

Figure 2. Test-bed rig

2.2 Electronics design

To support reliable operation, the system uses two ATmega328P microcontrollers with clearly separated responsibilities. The first ATmega328P is dedicated exclusively to real-time attitude stabilization, executing IMU data acquisition, sensor filtering, handling serial communication, and PID control at a fixed high update rate. These tasks require consistent timing and minimal CPU interruptions to maintain flight stability. The second ATmega328P processes GPS data and manages navigation-related tasks, which are computationally intermittent and can generate timing jitter due to variable GPS parsing loads. Because each ATmega328P provides only 16 MHz of processing speed and 2 KB of SRAM, combining both real-time control and GPS handling on a single unit would lead to resource saturation and potential delays in the control loop. By distributing the workload across two low-cost microcontrollers, the system ensures stable timing for attitude control, prevents GPS-induced interruptions, and improves overall reliability without requiring a more expensive high-performance processor.

The propulsion system consists of three Sunnysky V2216 800 KV rotors and one MG966R servomotor mounted on the tilt mechanism. Figure 3(a) presents the schematic diagram used for the tricopter's electronic system, while Figure 3(b) illustrates the graphical user interface (GUI) employed with a serial connection to simulate real-time sensor readings.

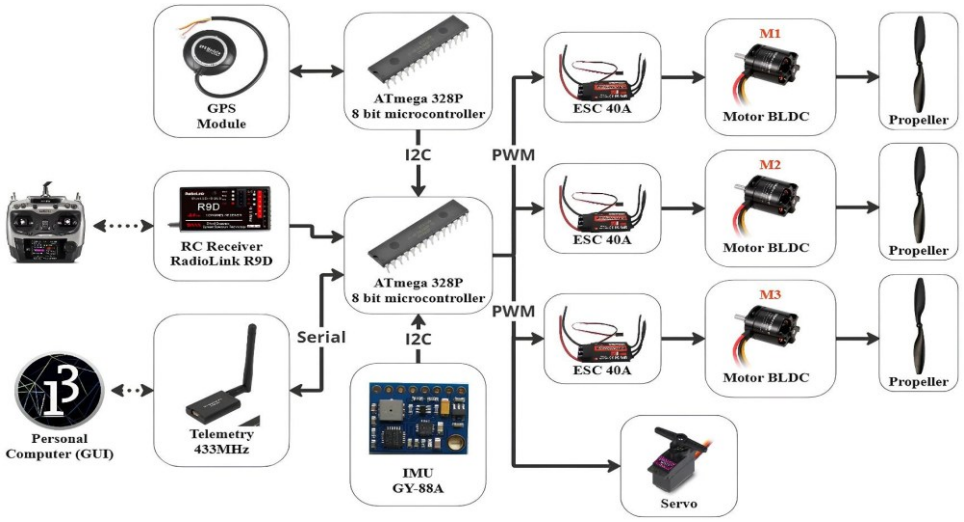

(a)

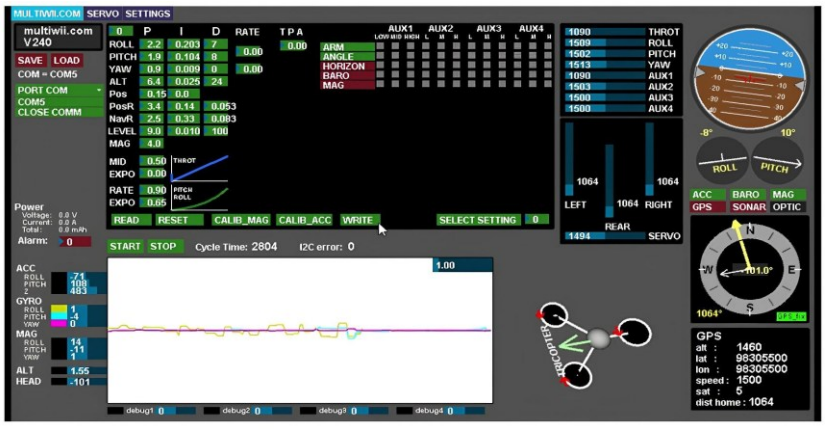

(b)

Figure 3. (a) Electronic system design, and (b) The GUI for tricopter sensor readings

Table 1 summarizes the main mechanical and electronic specifications of the proposed single-tilt-rotor tricopter platform. The system employs a lightweight Y-shaped carbon-fiber frame with a total mass of 1.3 kg and 225 mm arm length to achieve stable and agile flight performance. The propulsion system consists of three Sunnysky V2216 800 KV brushless motors equipped with 10×4.5-inch propellers and controlled by 40A ESCs, while yaw control is achieved using an MG966R servo motor mounted on the rear tilt mechanism. The flight control system utilizes two ATmega328P microcontrollers for real-time attitude stabilization and navigation, supported by a GY-88A IMU, GPS module, RadioLink R9D receiver, and 433 MHz telemetry communication. An 11.1 V, 5000 mAh battery powers the entire system, enabling low-cost, experimentally validated tricopter operation.

Table 1. Mechanical and electronic specifications of the proposed tricopter

Parameter	Specification	Parameter	Specification
UAV configuration	Single-tilt-rotor tricopter	Servo motor	MG966R
Frame configuration	Y-shaped frame	ESC	3 × ESC 40A
Total mass	1.3 kg	Battery	11.1 V 5000 mAh
Main platform dimensions	Width: 120–160 mm Length: 120–180 mm	Microcontroller	2 × ATmega328P (8-bit, 16 MHz)
Arm length	225 mm	IMU sensor	GY-88A
Center of gravity position	Geometric center of the frame	GPS module	GPS receiver module
Frame material	Carbon fiber	RC receiver	RadioLink R9D
Propeller size	Propeller 10 x 4.5 inches	Telemetry module	433 MHz telemetry
Brushless motor	3 × Sunnysky V2216 800 KV	GPS module	GPS receiver module

2.3 PID attitude control

Figure 4 illustrates the closed-loop attitude control architecture used to stabilize the tricopter during flight. The desired roll, pitch, and yaw references are compared with the measured attitude angles from the IMU sensor. The resulting attitude errors are processed by independent PID controllers for each rotational axis. The controller outputs are then distributed to the propulsion system through a motor-mixing mechanism that allocates control effort among the three BLDC motors and the tail-tilt servo actuator. The control signal flow begins with IMU-based attitude measurement, where the roll (ϕ), pitch (θ), and yaw (ψ) angles are estimated and fed back to the controller. The PID controller calculates the correction signal based on the error between the desired and measured attitude. These correction signals are subsequently converted into differential motor thrust commands to generate the required stabilization torques.

A PID controller was selected because of its low computational complexity, ease of implementation, and suitability for low-cost embedded systems [26][27][28]. Compared to advanced control strategies such as model predictive control (MPC), adaptive control, or nonlinear control approaches, PID control can operate reliably on the ATmega328P microcontroller with limited computational resources (16 MHz clock frequency and 2 KB SRAM), while still providing stable real-time attitude regulation. A comprehensive survey by Lozano et al. emphasizes that embedded aerospace platforms often prioritize computational simplicity and reliability over algorithmic complexity [29].

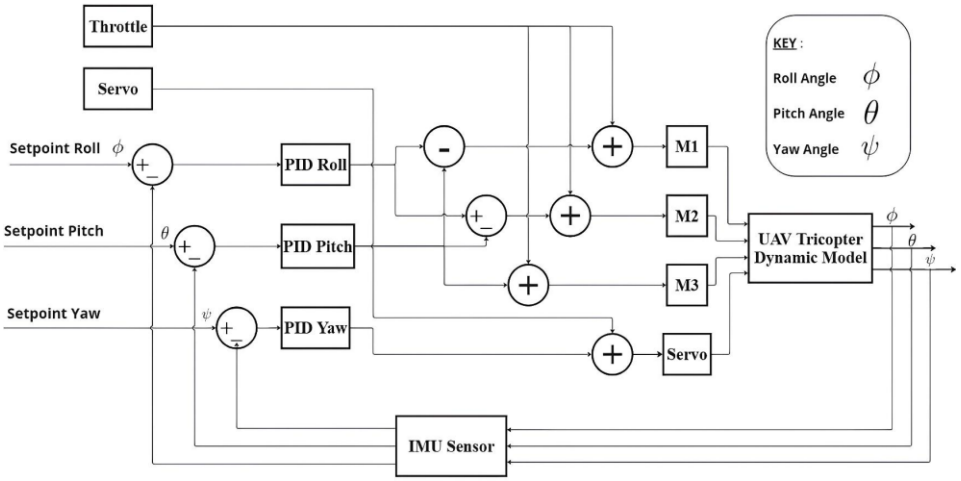

Figure 4. Control system block diagram for tricopter flight stability

For roll stabilization, the tricopter rotates about the longitudinal axis. To generate roll torque, differential thrust must be produced between the left and right rotors. As shown in Figure 5, when the tricopter tilts to the right, the controller increases the thrust of one motor while decreasing the thrust of the opposite motor to create a restoring torque. This differential thrust mechanism explains why the PID term is added to one motor and subtracted from the other. Assuming motors *M1* and *M2* are positioned symmetrically relative to the center of gravity, the generated roll torque can be approximated as in Equation (1).

$$\tau_{\phi} \propto l(F_{M2} - F_{M1}) \tag{1}$$

where l is the arm length and F_{M1}, F_{M2} are the thrusts generated by motors M1 and M2, respectively. Therefore, the roll control allocation is given by Equation (2).

$$\begin{aligned} Throttle_{M1} &= Throttle - PID_{\phi} \\ Throttle_{M2} &= Throttle + PID_{\phi} \\ Throttle_{M3} &= Throttle \end{aligned} \tag{2}$$

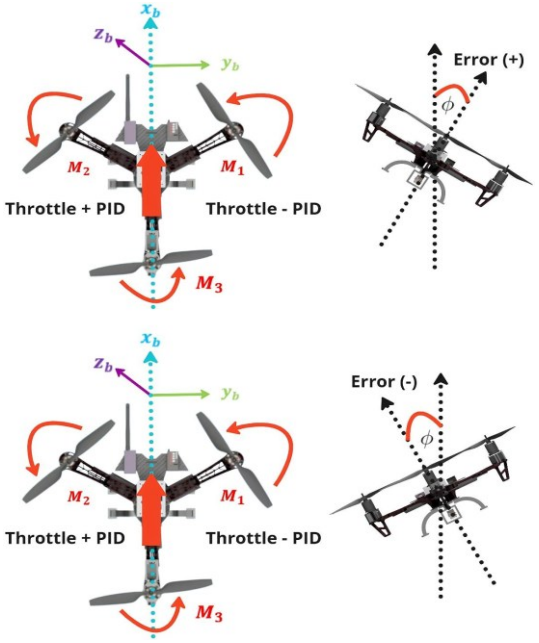

Figure 5. Tricopter attitude roll condition

As shown in Figure 6(a), forward motion results in a positive pitch error, whereas backward motion produces a negative pitch error. To stabilize the pitch angle, the PID controller adjusts the thrust distribution between the front motors (M1 and M2) and the rear motor (M3). Pitch motion is generated by creating a difference between the combined thrust of the front rotors and the thrust of the rear rotor. The resulting pitch torque can be approximated as in Equation (3).

$$\tau_\theta \propto l(F_{M3} - (F_{M1} + F_{M2})) \tag{3}$$

where l denotes the distance between the rotor and the center of gravity, while F_{M1}, F_{M2}, and F_{M3} represent the thrust generated by each motor, therefore, the PID controller modifies the motor throttle values to generate the restoring pitch moment required for stabilization. The pitch control allocation is expressed in Equation (4).

$$\begin{aligned} Throttle_{M1} &= Throttle - PID_\theta \\ Throttle_{M2} &= Throttle - PID_\theta \\ Throttle_{M3} &= Throttle + PID_\theta \end{aligned} \tag{4}$$

As shown in Figure 6(b), yaw motion is generated by the tilt-servo mechanism mounted on the rear rotor. Unlike roll and pitch stabilization, which are achieved through differential motor thrust, yaw control is produced by changing the direction of the rear rotor thrust using the servo actuator. When the servo tilts the rear rotor, a lateral thrust component is generated, producing a yaw torque about the vertical axis of the tricopter.

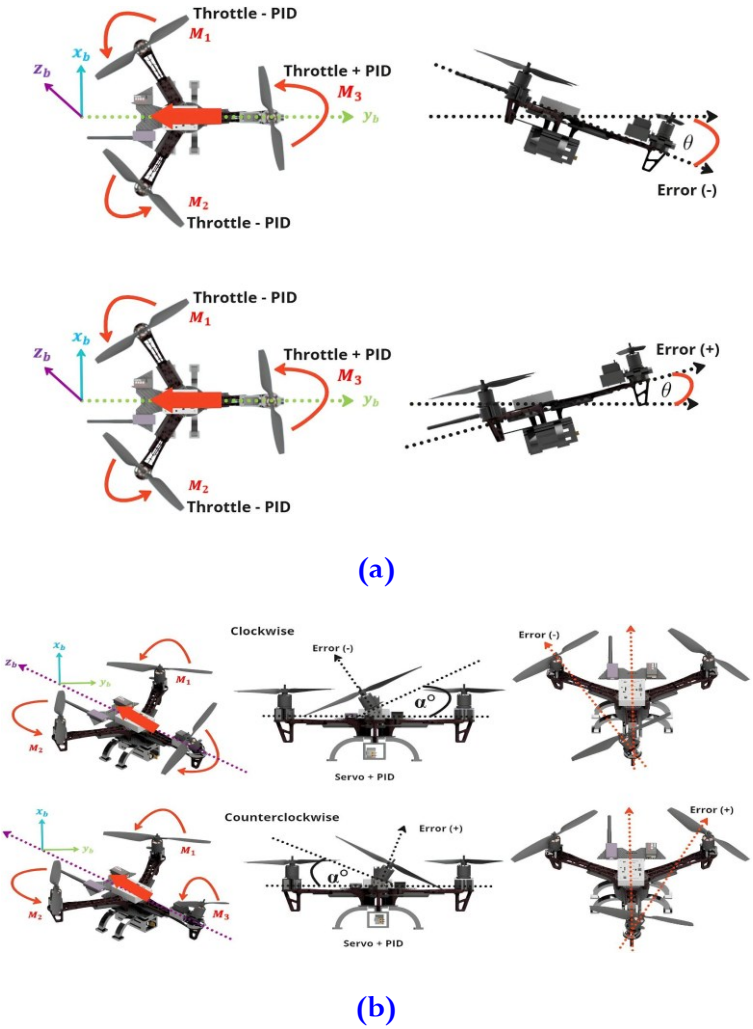

Figure 6. (a). Tricopter attitude pitch condition, and (b) Tricopter attitude yaw condition

During clockwise yaw motion, the servo tilts the rear rotor in one direction to generate a restoring yaw moment, whereas counterclockwise motion requires the opposite tilt direction. The generated yaw torque can be approximated as in Equation (5).

$$\tau_{\psi} \propto lF_{M3}\sin(\alpha) \tag{5}$$

where l is the distance from the rear rotor to the center of gravity, F_{M3} is the rear rotor thrust, and α is the servo tilt angle. Therefore, yaw stabilization is primarily achieved through servo angle adjustment rather than differential motor speed control. The PID controller adjusts the servo position based on the yaw error, as expressed in Equation (6).

$$\begin{aligned} Throttle_{M1} &= Throttle \\ Throttle_{M2} &= Throttle \\ Throttle_{M3} &= Throttle \\ Servo &= Servo + PID_{\psi} \end{aligned} \tag{6}$$

3. Results and discussion

3.1 Testing on the test-bed rig

Figure 7 shows the experimental setup used to test the tricopter attitude control. The PID control gains were obtained through manual tuning using the same test-bed rig under disturbance-free conditions, and the final gains are listed in Table 2. The controller was then validated experimentally by introducing disturbances in the form of fan-generated airflow. Two types of disturbances were applied: static noise and dynamic noise. The fan operated in three modes, and wind velocity was measured using an anemometer.

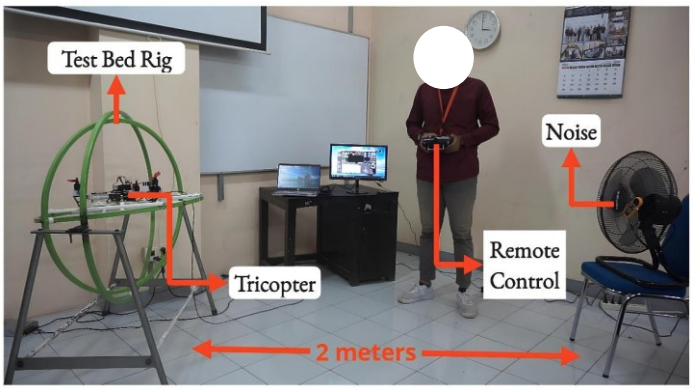

Figure 7. Tricopter test setup on a test-bed rig with wind noise. A video recording of the test results can be found at https://youtu.be/D2QHPibhbRI?si=6e0mie1vDKpjKDKJ

Table 2. PID control parameters for tricopter attitude during test-bed rig experiments

Parameters	Roll	Pitch	Yaw
Kp	2.2	1.8	4.4
Ki	0.203	0.203	0
Kd	7	6	14

For the static noise tests, three wind speeds were applied: 5 m/s, 6 m/s, and 7.2 m/s. Figure 8(a) illustrates the response to a 5 m/s disturbance. The roll and pitch angles experienced sudden deviations of about ±2°, followed by oscillatory behavior before returning to their nominal orientation within approximately 1 second, after which stability was maintained for 30 seconds.

At 6 m/s (Figure 8(b)), the roll angle oscillated between ±2°, while the pitch angle decreased by roughly 4° before gradually increasing until the 1000th sampling point (≈ 30 s). At 7.2 m/s (Figure 8(c)), the roll attitude experienced oscillatory deviations up to ±3°, while the pitch angle increased rapidly to about 7°. The mean absolute error (MAE) values for these tests are summarized in Table 3.

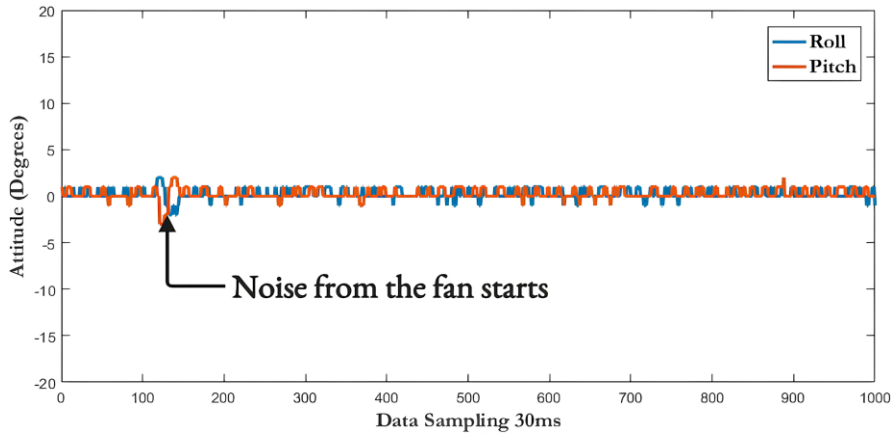

(a)

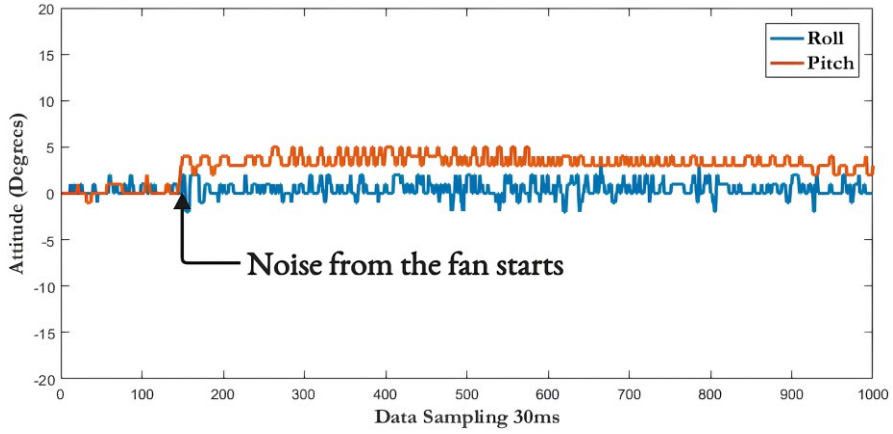

(b)

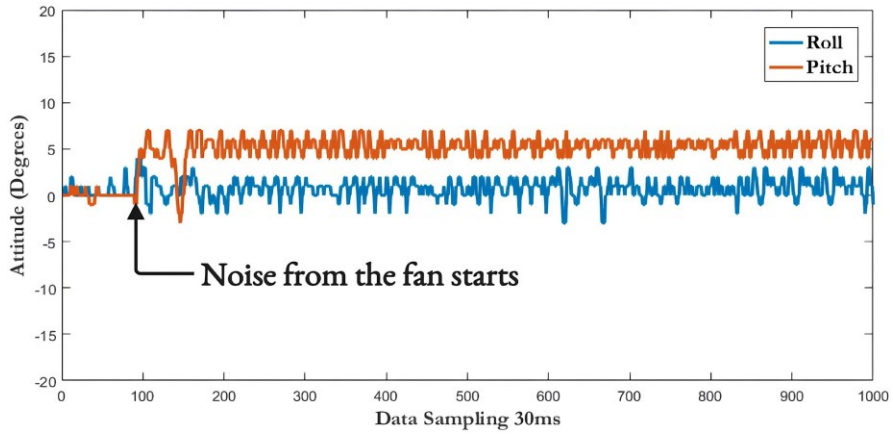

(c)

Figure 8. (a), Tricopter attitude response during static noise testing at 5 m/s, (b) Tricopter attitude response during static noise testing at 6 m/s, and (c) Tricopter attitude response during static noise testing at 7.2 m/s

Table 3. MAE of tricopter attitude during static noise testing

Attitude	Wind speed		
	5 m/s	6 m/s	7.2 m/s
Roll	0.345	0.621	0.977
Pitch	0.349	2.972	4.826

The data show that the pitch MAE increases more significantly with wind speed than the roll MAE, reflecting the asymmetric aerodynamic loading on the Y-frame structure. The yaw response is not analyzed in detail because the applied lateral wind disturbance predominantly affects the roll and pitch dynamics, while yaw motion is mainly governed by the tail-servo mechanism. In contrast to the static noise tests, the dynamic noise test used an oscillating fan with a maximum velocity of 7.2 m/s. Figure 9 shows the response, while Table 4 summarizes the MAE values. Because the fan oscillated, airflow was spread more widely, creating greater disturbances than in the static tests. Pitch disturbances reached up to $\pm 9^0$, while roll disturbances were also significant.

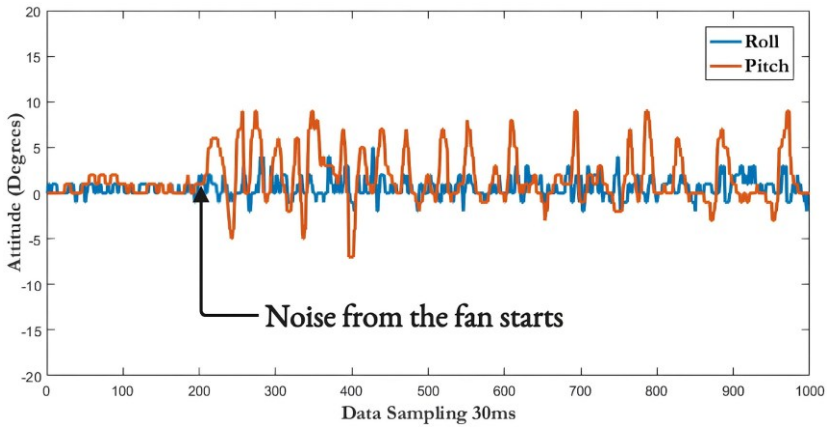

Figure 9. Tricopter attitude response during dynamic noise testing at 7.2 m/s

Table 4. MAE of tricopter attitude during dynamic noise testing at 7.2 m/s

Attitude	Wind speed 7.2 m/s
Roll	0.823
Pitch	2.094

Across all wind speeds, the pitch MAE is consistently higher than the roll MAE. This behavior arises from the inherent mechanical asymmetry of the single-tilt-rotor tricopter. Roll control is generated by differential thrust between the two front rotors, providing high-bandwidth and symmetric actuation. In contrast, pitch control depends on the rear tilt-servo mechanism, which introduces mechanical lag, internal servo deadband, and nonlinear coupling between pitch and yaw. Furthermore, the tricopter exhibits a slightly larger moment of inertia about the pitch axis due to the rear boom and battery placement, resulting in slower angular acceleration in response to wind disturbances.

3.2 Outdoor flight testing

Figure 10 shows the outdoor flight test setup, Figure 11 presents the roll and pitch responses, and Table 5 summarizes the corresponding MAE values. The results indicate that the MAE values obtained during outdoor flight are consistent with those measured using the test-bed rig. As observed earlier, the MAE for pitch is higher than that for roll, confirming that maintaining pitch stability at 0° is more challenging due to the asymmetric rear-tilt mechanism.

Figure 10. Tricopter outdoor flight testing

Table 5. MAE of tricopter attitude during flight testing

Attitude	Flight testing
Roll	1.133
Pitch	1.831

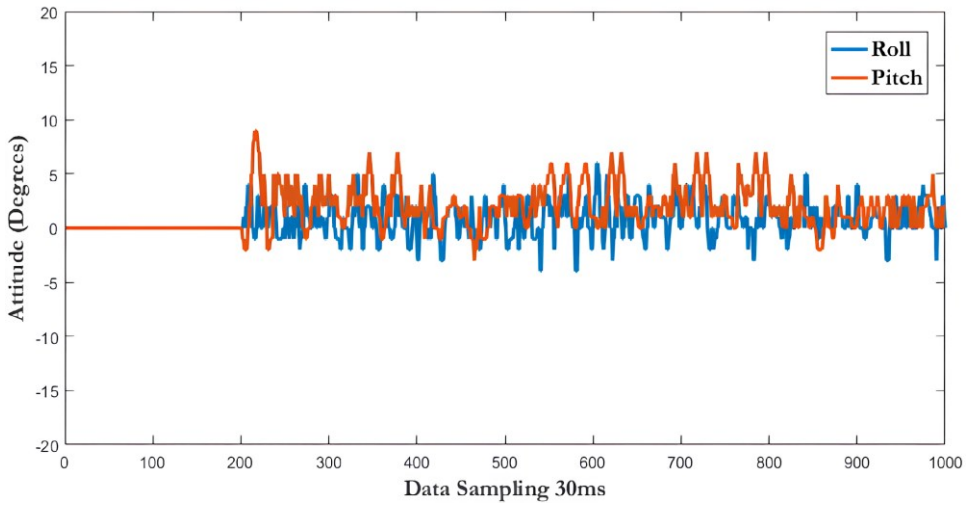

Figure 11. Attitude roll and pitch response during outdoor tricopter flight test

The outdoor MAE values fall between the static and dynamic-rig test results. This outcome is expected because the static rig provides idealized conditions with minimal aerodynamic interference. In contrast, the dynamic rig introduces combined rotational and translational airflow from the propellers, resulting in higher error. During outdoor flight, wind disturbances are present; however, the aircraft also benefits from aerodynamic damping and forward motion, which partially mitigates the disturbances. Consequently, the outdoor MAE values naturally lie between the static and dynamic rig performance.

3.3 Comparative discussion with existing controllers

Although the present work focuses on implementing a low-cost PID-based attitude controller on an ATmega328P-based tricopter platform, it is important to contextualize the obtained performance with respect to existing UAV control approaches reported in the literature. Table 6 summarizes representative control methods applied to tri-rotor and tri-tilt-rotor UAV systems.

Table 6. Comparison with the previous study

Controller type	Ref.	UAV Type	Performance	Notes
Nonlinear controller (nested saturation / backstepping-like)	[30]	Tri-rotor	Errors typically 2–5° under wind perturbations	First real-time nonlinear control implementation for tri-rotor
Nonlinear controller (stabilization)	[15]	Tri-rotor	Pitch/roll deviations 3–5° during aggressive motion	Strong robustness but computationally heavy
Linear Quadratic Regulator (LQR)	[17]	Tri-tilt-rotor	Tracking error < 3° in hover/translation experiments	Requires full-state measurement; not suitable for ATmega-class MCUs
Model Predictive Control (MPC)	[31]	Tri-tilt-rotor	Hovering attitude error < 2°	High computational demand; requires embedded PC or advanced MCU
Proposed PID (this study)	—	Tricopter	1.133° roll, 1.831° pitch (outdoor MAE)	Achieved using low-cost ATmega328P + GY-88A IMU

Note: Performance values for previous methods were taken from the respective referenced studies and may not be directly comparable due to differences in UAV configuration, operating conditions, disturbance profiles, hardware platforms, and evaluation metrics.

Previous studies have investigated various advanced control strategies for tricopter stabilization. Salazar-Cruz et al. [30] implemented a nonlinear controller for a tri-rotor UAV and demonstrated stable attitude regulation under disturbances. In another study, Salazar-Cruz et al. [15] proposed a nonlinear stabilization approach for a tri-rotor mini-aircraft and reported robust responses during aggressive maneuvers. Papachristos et al. [17] applied a Linear Quadratic Regulator (LQR)-based controller to a tri-tilt-rotor UAV to improve trajectory tracking performance, while Prach and Kayacan [31] proposed a Model Predictive Control (MPC)-based controller capable of achieving accurate hover stabilization and trajectory tracking.

As summarized in Table 6, the proposed PID controller achieves stable attitude control performance with outdoor MAE values of 1.133° for roll and 1.831° for pitch. These results fall within the performance range reported in previous tricopter and tilt-rotor UAV studies employing nonlinear, LQR, and MPC-based controllers. However, it should be noted that the reported values from the literature were obtained under different UAV platforms, hardware architectures, operating conditions, disturbance scenarios, and evaluation metrics. Therefore, the comparison presented in Table 6 is intended only as a qualitative contextual discussion, not a direct quantitative benchmark. Nevertheless, the comparison indicates that acceptable stabilization performance can still be achieved with a computationally lightweight PID controller implemented on a low-cost ATmega328P microcontroller. This demonstrates the practicality of the proposed approach for resource-constrained UAV systems where hardware simplicity, implementation cost, and real-time embedded execution are important considerations.

While the proposed system demonstrates stable experimental performance, several limitations should be acknowledged. The use of low-cost hardware introduces sensor noise, servo nonlinearities, and limited computational capability, which may affect performance during aggressive maneuvers or strong wind disturbances. The tail-tilt mechanism also introduces coupling

effects between yaw and pitch motion due to servo response limitations. Future work may investigate improved sensor fusion techniques, higher-performance embedded platforms, and adaptive or gain-scheduled control methods to enhance robustness and flight stability further. Overall, the experimental results demonstrate that the proposed low-cost PID-based tricopter system maintains stable attitude control under both static and dynamic wind disturbances. Despite the limited computational capability of the ATmega328P microcontroller, the controller achieved reliable stabilization performance during test-bed and outdoor flight experiments, confirming the feasibility of the proposed approach for low-cost UAV applications.

4. Conclusion

This study presented the design, implementation, and experimental validation of a low-cost single-tilt-rotor tricopter with a Y-shaped frame configuration and a servo-driven tail-tilt mechanism, controlled using a PID-based attitude controller implemented on an ATmega328P platform. The controller performance was evaluated experimentally using a test-bed rig under static and dynamic wind disturbances, as well as through outdoor flight testing. Under static wind disturbances up to 7.2 m/s, the roll and pitch MAE values reached 0.977° and 4.826°, respectively. Dynamic disturbance testing produced MAE values of 0.823° for roll and 2.094° for pitch, while outdoor flight tests resulted in MAE values of 1.133° for roll and 1.831° for pitch. The experimental results demonstrate that the proposed tricopter platform can maintain stable attitude control under both controlled disturbance conditions and real outdoor environments, despite being implemented on low-cost embedded hardware. Overall, the results confirm the feasibility of using a computationally lightweight PID controller to reliably stabilize resource-constrained tricopter systems. Future work will focus on adaptive PID tuning, improved sensor fusion, and extended flight testing under more complex real-world mission scenarios.

Author's declaration

Author contribution

Fahmizal: Conceptualization, Methodology. **Ahmad Jaelani Sidik**: Data curation, Formal analysis. **Priyova M. Rafief**: Software, Validation, Visualization. **Hari Maghfiroh**: Writing – review & editing. **Mariusz Jablonski** and **Piotr Borkowski**: Supervision.

Funding statement

This research was funded by the Universitas Sebelas Maret allocated from the 2026 Fiscal Year through the Fundamental Research A (PFA-UNS) scheme with the agreement number: 460/UN27.22/PT.01.03/2026.

Data availability

The data are available upon reasonable request from the corresponding author.

Acknowledgements

Not applicable

Competing interest

The authors declare that they are NOT affiliated with or involved in any organization or entity that has a financial interest (such as honoraria; educational grants; participation in speakers' bureaus;

membership, employment, consulting, stock ownership, or other equity interests; and expert testimony or patent licensing arrangements), or non-financial interest (such as personal or professional relationships, affiliations, knowledge, or beliefs) in the subject matter or materials discussed in this manuscript.

Ethical clearance

Not applicable

AI statement

During the preparation of this manuscript, the authors used ChatGPT solely to improve language, readability, and writing clarity. All AI-generated suggestions were carefully reviewed, revised, and validated by the authors, who take full responsibility for the content of this publication. In addition, the manuscript underwent comprehensive proofreading and language editing by an English-language expert to enhance grammar, clarity, coherence, and the quality of academic writing. Neither the AI tool nor the language editing process influenced the scientific content, methodology, data analysis, results, or conclusions of the study.

Publisher's and Journal's note

Universitas Negeri Padang as the publisher, and Editor of Teknomekanik state that there is no conflict of interest towards this article publication.

References

[1] H. Maghfiroh, C. Hermanu, and V. Sitorini Zul Hizmi, "Position Control of Vtol System Using Anfis Via Hardware in the Loop," *Sinergi*, vol. 25, no. 3, p. 309, 2021, https://doi.org/10.22441/sinergi.2021.3.008

[2] M. A. Al-bahrany and A. T. A. Sadda, "Smart DC to DC Converter for a Small Drone Based Deep Learning Technique," *Journal of Fuzzy Systems and Control*, vol. 1, no. 2, pp. 55–60, 2023, https://doi.org/10.59247/jfsc.v1i2.43

[3] Fahmizal, D. Yanu Kharisma, and S. Pramono, "Implementation of Fuzzy Logic Control on a Tower Copter," *Journal of Fuzzy Systems and Control*, vol. 1, no. 1, pp. 14–17, 2023, https://doi.org/10.59247/jfsc.v1i1.25

[4] S. Lee, D. Har, and D. Kum, "Drone-Assisted Disaster Management: Finding Victims via Infrared Camera and Lidar Sensor Fusion," in *APWC on CSE/APWCE 2016*, IEEE, 2017, pp. 84–89. https://doi.org/10.1109/APWC-on-CSE.2016.025

[5] T. Villa, F. Gonzalez, B. Miljevic, Z. D. Ristovski, and L. Morawska, "An overview of small unmanned aerial vehicles for air quality measurements: Present applications and future prospectives," *Sensors (Switzerland)*, vol. 16, no. 7, pp. 12–20, 2016, https://doi.org/10.3390/s16071072

[6] B. H. Prasetio, A. A. Supianto, G. E. Setiawan, B. D. Setiawan, I. Cholissodin, and S. R. Akbar, "Earth image classification design using unmanned Aerial vehicle," *Telkomnika (Telecommunication Computing Electronics and Control)*, vol. 13, no. 3, pp. 1021–1028, 2015, https://doi.org/10.12928/telkomnika.v13i3.1786

[7] M. M. Marques *et al.*, "GammaEx project: A solution for CBRN remote sensing using unmanned aerial vehicles in maritime environments," *OCEANS 2017 - Anchorage*, vol. 2017-Janua, pp. 1–6, 2017. https://ieeexplore.ieee.org/document/8232258

[8] H. Maghfiroh, C. Hermanu, A. W. Rilo Pambudi, J. S. Saputro, F. Adriyanto, and M. Nizam, "Position Control Using Linear Quadratic Gaussian on Vertical Take-Off Landing,"

3rd 2021 East Indonesia Conference on Computer and Information Technology, EIConCIT 2021, pp. 260–264, 2021, https://doi.org/10.1109/EIConCIT50028.2021.9431866

[9] Fahmizal, D. Afidah, S. Istiqphara, and N. S. Abu, "Interface Design of DJI Tello Quadcopter Flight Control," *Journal of Fuzzy Systems and Control*, vol. 1, no. 2, pp. 49–54, 2023, https://doi.org/10.59247/jfsc.v1i2.35

[10] F. Jiang, F. Pourpanah, and Q. Hao, "Design, Implementation, and Evaluation of a Neural-Network-Based Quadcopter UAV System," *IEEE Transactions on Industrial Electronics*, vol. 67, no. 3, pp. 2076–2085, 2020, https://doi.org/10.1109/TIE.2019.2905808

[11] J. I. Giribet, R. S. Sánchez-Peña, and A. S. Ghersin, "Analysis and design of a tilted rotor hexacopter for fault tolerance," *IEEE Trans. Aerosp. Electron. Syst.*, vol. 52, no. 4, pp. 1555–1567, 2016, https://doi.org/10.1109/TAES.2016.140885

[12] T. P. Nascimento and M. Saska, "Position and attitude control of multi-rotor aerial vehicles: A survey," *Annu. Rev. Control*, vol. 48, pp. 129–146, 2019, https://doi.org/10.1016/j.arcontrol.2019.08.004

[13] J. Escareño, A. Sanchez, O. Garcia, and R. Lozano, "Triple tilting rotor mini-UAV: Modeling and embedded control of the attitude," in *Proceedings of the American Control Conference*, 2008, pp. 3476–3481. https://doi.org/10.1109/ACC.2008.4587031

[14] M. S. Atif, Z. Haider, M. M. Zohaib, and M. A. Raza, "Embedded and Control Systems Design and Implementation of T-Shaped Tilt-Rotor Tri-copter," in *2021 7th International Conference on Control Science and Systems Engineering, ICCSSE 2021*, IEEE, 2021, pp. 78–82. https://doi.org/10.1109/ICCSSE52761.2021.9545147

[15] S. Salazar-Cruz, R. Lozano, and J. Escareño, "Stabilization and nonlinear control for a novel trirotor mini-aircraft," *Control Eng. Pract.*, vol. 17, no. 8, pp. 886–894, 2009, https://doi.org/10.1016/j.conengprac.2009.02.013

[16] D. A. Ta, I. Fantoni, and R. Lozano, "Modeling and control of a tilt tri-rotor airplane," *Proceedings of the American Control Conference*, pp. 131–136, 2012, https://doi.org/10.1109/acc.2012.6315155

[17] C. Papachristos, K. Alexis, and A. Tzes, "Linear quadratic optimal trajectory-tracking control of a longitudinal thrust vectoring-enabled unmanned Tri-TiltRotor," *IECON Proceedings (Industrial Electronics Conference)*, pp. 4174–4179, 2013, https://doi.org/10.1109/IECON.2013.6699805

[18] A. Rys, R. Czyba, and G. Szafranski, "Development of control system for an unmanned single tilt tri-rotor aerial vehicle," *2014 International Conference on Unmanned Aircraft Systems, ICUAS 2014 - Conference Proceedings*, pp. 1091–1098, 2014, https://doi.org/10.1109/ICUAS.2014.6842361

[19] I. Jannasch and D. Sabatta, "Design and construction of a self-levelling tricopter using gain scheduling and PID controllers," *Proceedings - 2019 Southern African Universities Power Engineering Conference/Robotics and Mechatronics/Pattern Recognition Association of South Africa, SAUPEC/RobMech/PRASA 2019*, pp. 56–61, 2019, https://doi.org/10.1109/RoboMech.2019.8704801

[20] K. J. Nam, J. Joung, and D. Har, "Tri-Copter UAV with Individually Tilted Main Wings for Flight Maneuvers," *IEEE Access*, vol. 8, pp. 46753–46772, 2020, https://doi.org/10.1109/ACCESS.2020.2978578

[21] J. A. Bautista, A. Osorio, and R. Lozano, "Modeling and analysis of a tricopter/flying-wing convertible UAV with tilt-rotors," *2017 International Conference on Unmanned Aircraft Systems, ICUAS 2017*, pp. 672–681, 2017, https://doi.org/10.1109/ICUAS.2017.7991502

[22] S. Jatsun, O. Emelyanova, A. S. M. Leon, and S. Stykanyova, "Control fligth of a UAV type tricopter with fuzzy logic controller," *11th International IEEE Scientific and Technical Conference "Dynamics of Systems, Mechanisms and Machines", Dynamics 2017 - Proceedings*, vol. 2017-Novem, pp. 1–5, 2017, https://doi.org/10.1109/Dynamics.2017.8239459

[23] A. Prach and E. Kayacan, "An MPC-based position controller for a tilt-rotor tricopter VTOL UAV," *Optim. Control Appl. Methods*, vol. 39, no. 1, pp. 343–356, 2018, https://doi.org/10.1002/oca.2350

[24] M. Mehndiratta and E. Kayacan, "Online Learning-based Receding Horizon Control of Tilt-rotor Tricopter: A Cascade Implementation," *Proceedings of the American Control Conference*, vol. 2018-June, pp. 6378–6383, 2018, https://doi.org/10.23919/ACC.2018.8430814

[25] M. Jabłoński and P. Borkowski, "Correction Mechanism for Balancing Driving Torques in an Opencast Mining Stacker with an Induction Motor and Converter Drive System," *Energies (Basel).*, vol. 15, no. 4, 2022, https://doi.org/10.3390/en15041282

[26] H. Maghfiroh, M. Nizam, and S. Praptodiyono, "PID optimal control to reduce energy consumption in DC-drive system," *International Journal of Power Electronics and Drive Systems*, vol. 11, no. 4, pp. 2164–2172, 2020, https://doi.org/10.11591/ijpeds.v11.i4.pp2164-2172

[27] H. Maghfiroh, O. Wahyunggoro, A. I. Cahyadi, and S. Praptodiyono, "PID-hybrid tuning to improve control performance in speed control f DC motor base on PLC," *Proceedings of 2013 3rd International Conference on Instrumentation, Control and Automation, ICA 2013*, no. August, pp. 233–238, 2013, https://doi.org/10.1109/ICA.2013.6734078

[28] H. Maghfiroh, I. Iftadi, and A. Sujono, "Speed control of induction motor using lqg," *Journal of Robotics and Control (JRC)*, vol. 2, no. 6, pp. 565–570, 2021, https://doi.org/http://doi.org/10.18196/jrc.26138

[29] S. Ahmed khan *et al.*, "Active attitude control for microspacecraft; A survey and new embedded designs," *Advances in Space Research*, vol. 69, no. 10, pp. 3741–3769, 2022, https://doi.org/10.1016/j.asr.2022.02.020

[30] S. Salazar-Cruz, F. Kendoul, R. Lozano, and I. Fantoni, "Real-time stabilization of a small three-rotor aircraft," *IEEE Trans. Aerosp. Electron. Syst.*, vol. 44, no. 2, pp. 783–794, 2008, https://doi.org/10.1109/TAES.2008.4560220

[31] C. Papachristos, K. Alexis, and A. Tzes, "Model predictive hovering-translation control of an unmanned Tri-TiltRotor," *Proc. IEEE Int. Conf. Robot. Autom.*, pp. 5425–5432, 2013, https://doi.org/10.1109/ICRA.2013.6631355